Mechanics Transport Communications

ISSN 1312-3823 (print)
ISSN 2367-6620 (online)
volume 22, issue 3/3, 2024
Academic journal **http://www.mtc-aj.com** **article № 2601**

OPTIMIZATION OF ANTI-SLIPPROTECTION BASED ON RESULTS SIMULATION OF TORSIONAL MOMENT ON THE DRIVE AXLES OF SERIES ŽS 444 LOCOMOTIVES OF SERBIA RAILWAYS

Branislav Gavrilovic[1)], Bundalo Zoran[2)]
gavrilovicbranislav5@gmail.com, cheminot2@gmail.com

[1,2)] Belgrade Academy of Technical and Art Applied Studies,
Department: School of Railway Transport
SERBIA

Key words: *railway traction vehicles, mechanical resonance, locomotives of the ŽS 444 series*

Abstract: *The appearance of mechanical resonance in the axle assembly of railway traction vehicles with motors for DC wave current has been the subject of interest of railway experts for a long time. This is not accidental, considering that the resonance is usually accompanied by cracks and breaks in certain parts of the axle assembly, thus endangering railway traffic. Despite a series of previous researches, during the reconstruction and modernization of railway traction vehicles, the impact of changing diode rectifier devices with semi-controllable asymmetric thyristor ones, such as those found in ŽS 444 series locomotives, has not been fully considered. This study aimed to review the impact of electrical parameters, primarily the effect of the rectified voltage and current supplied to the traction motors on the size and shape of the torsional moments on the drive shaft. On the basis of the conducted analysis, the anti-skid protection of locomotives of the ŽS 444 series was optimized, i.e. protective measures were proposed that are also relevant for other series of electric traction vehicles in the "Serbian Railways" inventory park (ŽS 441 and ŽS 461).*

1. INTRODUCTION

As part of the main overhaul of thirty locomotives of the ŽS 441 series during 2006/07. In 2010, modifications were made primarily to the electrical equipment of the locomotive in order to increase the traction capabilities of the vehicle, increase the reliability in operation and ensure better conditions for the work of the traction and maintenance staff. During the modification, the high-voltage regulation switch was removed because the diode uncontrollable rectifier was replaced with a thyristor semi-controllable one. The traction circuit is actually designed so that the traction motors with the associated equipment are divided into two identical two-motor groups (Figure 1). The first two-motor group was axles have equal adhesion conditions. Within each two-motor group, traction motors with associated components (rectifier, choke) are connected in series.

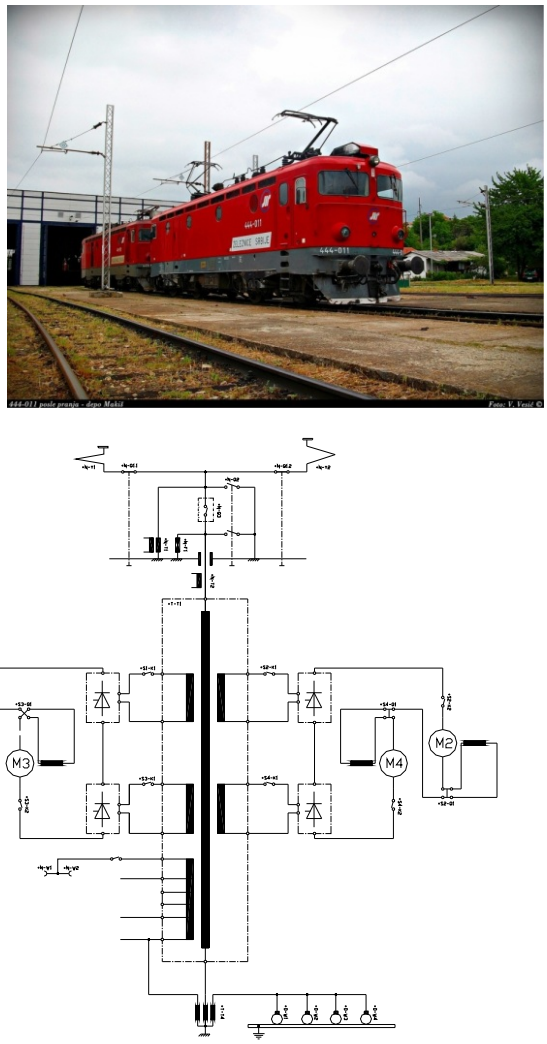

Fig. 1: Appearance and simplified diagram of the traction circuit of the locomotive JŽ 444

Anti-slip protection of electric locomotives with DC traction motors for wave current such as ŽS 444 series locomotives is, in principle, slightly different from this protection in other locomotives [1]. This protection is mainly based on the timely detection of slippage by means of appropriate sensors, the automatic weakening of the traction forces of the drive axles and the increase of adhesion conditions by sandblasting between the wheel and the rail. However, despite the series of locomotive shaft fractures, previous researches did not give a precise answer to how effective anti-skid protection is and for what period of time it must react [2].

In order to achieve optimal anti-skid protection for these locomotives, the influence of the change in voltage and current supplied to traction motors for direct wave current on the occurrence of resonance, i.e. the size and shape of torsional moments on the drive shafts, will first be considered. This impact will be evaluated using a simulation model of the ŽS 444 series locomotive axle assembly in Matlab-Cimulink.

2. MECHANICAL RESONANCE OF THE LOCOMOTIVE DRIVE SYSTEM

The drive system of electric traction vehicles of the ŽS 444 series is a mechanical system consisting of a traction electric motor for DC wave current (3), gear coupling (2), torsion shaft (5), rubber coupling, reducer (1), drive shafts (4) and monobloc wheels (Figure 2) [3,4].

The basic movement of the system is rotation with the transmission of drive torque from the motor shaft to the monoblock wheels. Until now, research shows that in addition to rotation in the system, large and dangerous torsional oscillations of the drive shafts can occur, which as a rule lead to cracks and breaks in the drive shafts [3,4].

In order to define the dynamic behavior of the axle assembly of the ŽS 444 series locomotives, first of all, the instantaneous values of the torque M and the angular velocity ω on the motor shaft will be related to the traction force F_v, the vehicle speed v and the traction resistances $\sum F_{ot}$.

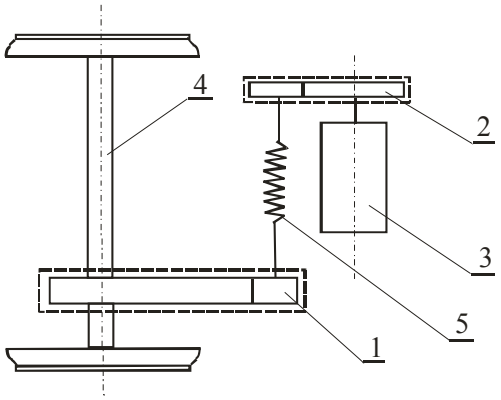

Fig. 2: Transmission of engine torque to drive shafts

With the indicated markings, the dynamic balance equation on the electric motor shaft is [3,4]:

$$J_m \frac{d\omega}{dt} = M - M_m \quad ...(1)$$

wherein:

Jm – moment of inertia of all rotating masses rotating at angular speed ω . For the analyzed case, it is: the moment of inertia of the driving electric motor of $550\ Nms^2$, of the gear coupling of $2\ Nms^2$, of the torsion shaft of $3Nms^2$, of the rubber coupling of $10\ Nms^2$ and of the smaller gear of the reducer $10\ Nms^2$, i.e. $J_m = 575\ Nms^2$ [5];

ω – angular speed of rotation of the electric motor shaft.

M(t) – current value of torque on the motor shaft,

Mm(t) - the current value of the torque with which the power transmission acts on the motor rotor,

D – diameter of the rolling circle of the driving wheels (D=1210 mm),

i- transmission ratio of the gear reducer ($i = 3,65$).

Figure 3 shows the direction of action of the driving torque M0 which originates from the traction force $\vec{F}'_v$ and the torque Mv from the reaction force of the ground on the wheel $\vec{F}_v$ ($\vec{F}_v = -\vec{F}'_v$). In the same Figure 3, the moment of inertia of all rotating masses rotating at the angular velocity of the locomotive shaft ω0 is marked with J0. For the analyzed case, it is: the moment of inertia of the large gear of $1600\ Nms^2$, of the drive shaft of $340\ Nms^2$ and of the monobloc wheels of $1600\ Nms^2$, i.e. $J_0 = 2120\ Nms^2$ [5].

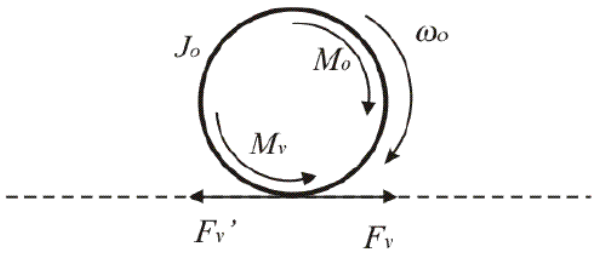

Fig. 3. Display of forces and moments acting on the wheel during vehicle movement

For the system shown in Figure 3, the dynamic equilibrium equation is:

$$J_0 \frac{d\omega_0}{dt} = M_0 - M_v \quad ...(2)$$

Since the:

$$\omega_0 = \frac{2}{D} \cdot v = \frac{\omega}{i} \quad ...(3)$$

$$M_0 = \eta \cdot i \cdot M_m \quad ...(4)$$

$$M_v = \frac{D}{2} \cdot F_v \quad ...(5)$$

wherein:

η - degree of useful effect, which according to the provisions of IEC - 349 is on average 0.975.

Based on equations (1) and (4), we have:

$$J_m \frac{d\omega}{dt} = M - \frac{M_0}{\eta \cdot i}$$

$$J_m \frac{d}{dt}\left(\frac{\omega}{\omega_n}\right) = \frac{M_n}{\omega_n}\left(\frac{M}{M_n} - \frac{1}{\eta \cdot i} \cdot \frac{M_0}{M_n}\right)$$

$$J_m \frac{d\omega_*}{dt} = \frac{M_n}{\omega_n}\left(M_* - M_{0*}\right) ...(6)$$

wherein:

$$M_{0b} = M_{0n} = \eta \cdot i \cdot M_n = 0{,}975 \cdot 3{,}65 \cdot 7846{,}824 = 27924{,}8849 \ Nm$$

Based on equations (2) and (5), we have:

$$J_0 \frac{d\omega_0}{dt} = M_0 - \frac{D}{2} \cdot F_v ...(7)$$

The equation of motion of the axle assembly of the vehicle is:

$$m \frac{dv}{dt} = F_v - \sum F_{ot} \quad ... (8)$$

wherein:

m - vehicle mass per one axle (20 t);

$\sum F_{ot}$ - the total force of resistance to movement between the wheel and the rail (forces: rolling friction on the surface; friction in the bearings; air resistance; climbing resistance; bending and inertial forces).

Based on the previous equations, we get:

$$F_v = m \frac{D}{2} \frac{d\omega_0}{dt} + \sum F_{ot}$$

$$J_0 \frac{d\omega_0}{dt} = M_0 - m\left(\frac{D}{2}\right)^2 \frac{d\omega_0}{dt} - \frac{D}{2}\sum F_{ot}$$

$$\left(J_0 + m\cdot\left(\frac{D}{2}\right)^2\right)\frac{d\omega_0}{dt} = M_0 - \frac{D}{2}\sum F_{ot} \text{ ...(20)}$$

$$\left(J_0 + m\cdot\left(\frac{D}{2}\right)^2\right)\frac{d}{dt}\left(\frac{\omega_0}{\omega_{0n}}\right) = \frac{M_{0n}}{\omega_{0n}}\left(\frac{M_0}{M_{0n}} - \frac{M_{Fv}}{M_{0n}}\right)$$

$$\left(J_0 + m\cdot\left(\frac{D}{2}\right)^2\right)\frac{d\omega_{0*}}{dt} = \frac{M_{0n}}{\omega_{0n}}\left(M_{0*} - M_{Fv*}\right)\text{...(9)}$$

wherein:

$\omega_{0n} = \frac{\omega_n}{i} = \frac{130,83}{3,65} = 35,8438\frac{rad}{s}$;

$M_{Fv*} = \frac{\frac{D}{2}\Sigma F_{ot}}{M_{0n}}$ - the relative value of the traction resistance moment. Considering the available adhesion mass at the adhesion friction coefficient of the locomotive of $\mu = 0,33$:

$$M_{Fv*} = \frac{\frac{D}{2}\Sigma F_{ot}}{M_{0n}} < \frac{39930}{27924,8849} = 1,43\,r.j$$

For equations (17) and (20) we have that in the complex domain:

$$\omega = \frac{M_n\cdot\left(M_* - M_{0*}\right)}{J_m\cdot\omega_n\cdot s} \text{ ...(10)}$$

$$\omega_0 = \frac{M_{0n}\left(M_{0*} - M_{Fv*}\right)}{\left(J_0 + m\left(\frac{D}{2}\right)^2\right)\cdot\omega_{0n}\cdot s} \text{ ...(11)}$$

The torsion moment of the locomotive shaft is:

$M_t = k\cdot\Delta\theta$.. (12)

$\Delta\theta = \frac{1}{i}\theta - \theta_0$

$\omega_0 = \frac{d\theta_0}{dt}$, and in the complex domain $\theta_0 = \frac{\omega_0}{s}$ ...(13)

$\omega = \frac{d\theta}{dt}$, and in the complex domain $\theta = \frac{\omega}{s}$ ...(14)

wherein:

k - torsional constant of the locomotive shaft. The torsional moment of the locomotive shaft is calculated separately for the shorter part k_1 and the longer part of the shaft k_2. For the shorter part of the shaft, i.e. between the gears of the reducer and the closer monobloc wheel, the torsion constant is $k_1 = 553\cdot10^6\,Nm\cdot rad^{-1}$, and for the longer part of the shaft $k_2 = 9,8\cdot10^6\,Nm\cdot rad^{-1}$ [5];

θ - angle of rotation of the locomotive shaft due to the action of the driving torque;

θ_0 - the turning angle of the locomotive shaft due to the reaction of the ground to the wheel.

2.1 Resonant frequency of the drive system

Since the:

$$\theta_0 = \frac{\frac{k}{i}}{\left(J_0 + m \cdot \left(\frac{D}{2}\right)^2\right) \cdot s^2 + k} \theta \quad ...(15)$$

Solving this equation gives:

The transfer function of the observed mechanical system W_t that connects the torque on the engine shaft M and the torsional torque on the driving axles of the locomotive M_t is:

$$W_t = \frac{M_t}{M} = \frac{1}{\left(J_m \cdot k + \frac{k}{\eta \cdot i^2}\left(J_0 + m \cdot \left(\frac{D}{2}\right)^2\right)\right) \cdot s^2} \cdot \frac{\frac{k}{i}\left(J_0 + m \cdot \left(\frac{D}{2}\right)^2\right) \cdot s^2}{\left(\frac{J_m \cdot \left(J_0 + m \cdot \left(\frac{D}{2}\right)^2\right)}{J_m \cdot k + \frac{k}{\eta \cdot i^2}\left(J_0 + m \cdot \left(\frac{D}{2}\right)^2\right)} \cdot s^2 + 1\right)} \quad ...(17)$$

The dominant poles of the transfer function W_t define the resonant frequency of the shaft assembly. Resonance frequencies for the shorter and longer part of the shaft from the gear to the monobloc wheel are determined by the general equation:

$$\omega = \sqrt{\frac{J_m \cdot k + \frac{k}{\eta \cdot i^2}\left(J_0 + m \cdot \left(\frac{D}{2}\right)^2\right)}{J_m \cdot \left(J_0 + m \cdot \left(\frac{D}{2}\right)^2\right)}} \quad ...(18)$$

Based on equation (18), for the shorter or longer part of the shaft from the gear to the monoblock wheel, the resonance frequencies are:

$$\omega_1 = \sqrt{\cdot 55310^6} \sqrt{\frac{575 + \frac{1}{0{,}975 \cdot 3{,}65} \cdot \left(2120 + 200000 \cdot \left(\frac{1{,}21}{2}\right)^2\right)}{575 \cdot \left(2120 + 200000 \cdot \left(\frac{1{,}21}{2}\right)^2\right)}}$$

$$\omega_1 = 526{,}87 \frac{rad}{s} \quad ...(19)$$

$$\omega_2 = \sqrt{\cdot 9{,}810^6} \sqrt{\frac{575 + \frac{1}{0{,}975 \cdot 3{,}65} \cdot \left(2120 + 200000 \cdot \left(\frac{1{,}21}{2}\right)^2\right)}{575 \cdot \left(2120 + 200000 \cdot \left(\frac{1{,}21}{2}\right)^2\right)}}$$

$$\omega_2 = 70{,}14 \frac{rad}{sec} \quad ...(20)$$

3. SIMULATION OF THE DRIVE SYSTEM IN MATLAB-SIMULINK

In the locomotives of the ŽS 444 series, the automatic regulation of the operation of traction electric motors was realized by means of the application of cascade feedback according to electric current and fast rotation [10-16]. The propulsion system of the locomotive driven by this regulated electric motor is shown in Figure 4.

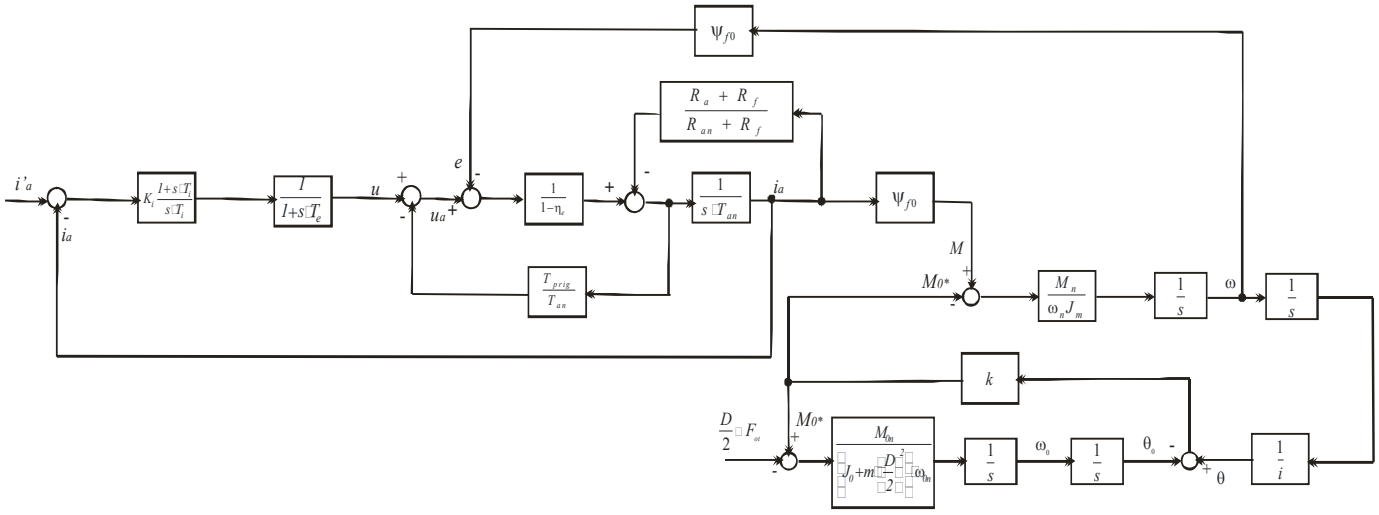

$$\theta = \frac{\left(\left(J_0 + m\cdot\left(\frac{D}{2}\right)^2\right)\cdot s^2 + k\right)}{J_m\cdot\left(J_0 + m\cdot\left(\frac{D}{2}\right)^2\right)\cdot s^4 + \left(J_m\cdot k + \frac{k}{\eta\cdot i^2}\left(J_0 + m\cdot\left(\frac{D}{2}\right)^2\right)\right)\cdot s^2}\cdot M \quad ...(16)$$

Fig. 4: Dynamic model of the locomotive drive system with an automatically regulated electric motor by electric current and rotation speed

wherein:

$W_{fil} = \frac{1}{1 + s\cdot T_e}$ - the transfer function of the measuring filter of the electric motor, which was determined by the method of symmetrical optimum with the selected damping coefficient of ζ=0.707 and $T_e = 0{,}002r.j$;

$W_i = K_i\cdot\frac{1 + s\cdot T_i}{s\cdot T_i}$ - the transfer function of the current regulator, which is determined by the

$W_\omega = K_\omega\cdot\frac{1 + s\cdot T_\omega}{s\cdot T_\omega}$ - the transfer function of the angular velocity regulator where: $T_\omega = 0{,}0812r.j$ and $K_\omega = 16{,}01$.

Based on the dynamic model in Figure 4, a simulation program was created in Matlab-Simulink as in Figure 5.

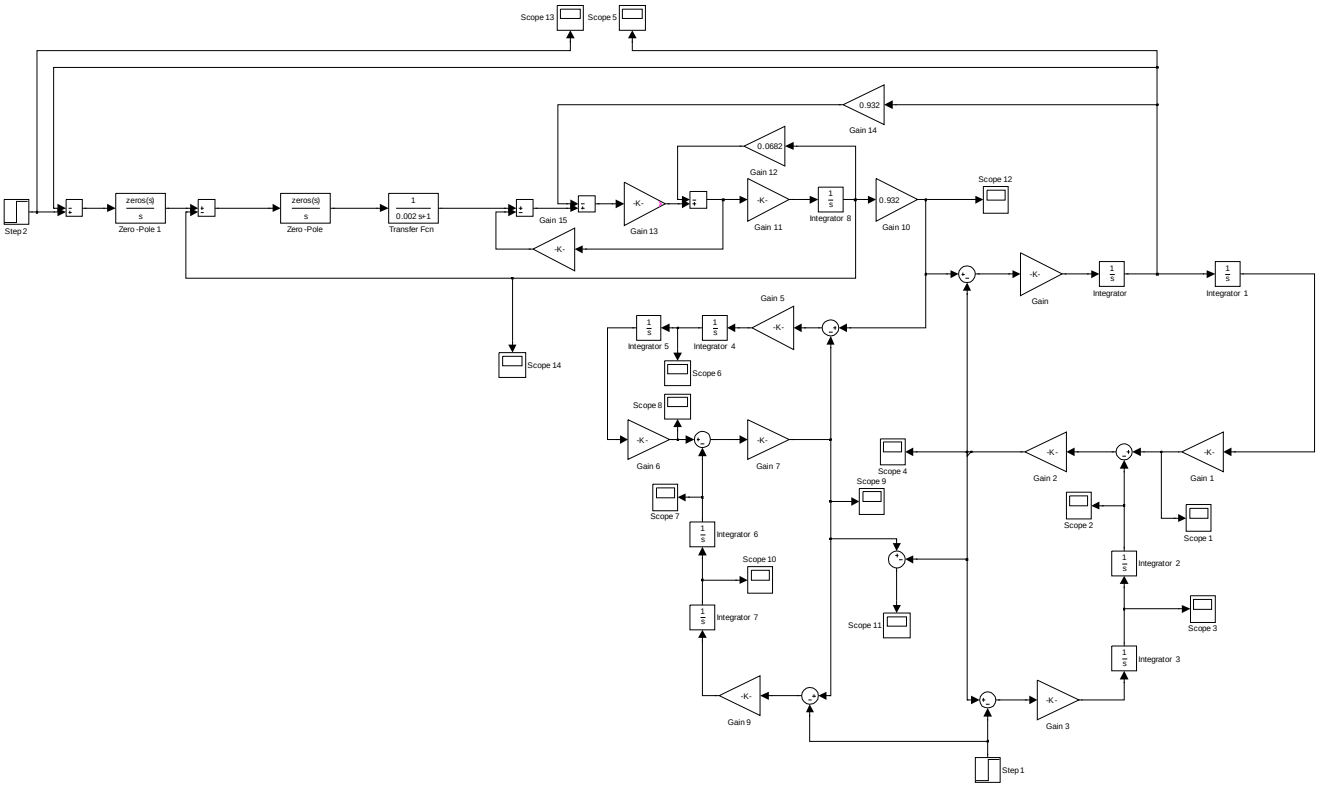

Fig. 5: Model of the locomotive drive system in Matlab-Simulink

As past experiences show that when the wheels start and slip on the railway track due to poor athesiological conditions, individual parts of the observed drive system may break, so in this work, special attention is paid to the analysis of just such a mode of operation of the locomotive [2].

In order to analyze the mentioned mode of operation, it is assumed that due to wet, dirty or greasy rails, the slippage of the axle assembly occurred at traction resistances that are equal to the rated torque of the electric motor, i.e. when $M_{Fv^*} = \dfrac{\dfrac{D}{2}\Sigma F_{ot}}{M_{0n}} = 1$: due to reduction of athesia coefficient below $\mu < 0{,}23$. (This value is determined from the condition: $F_v > \mu \cdot Q_a \Rightarrow \mu < \dfrac{M_{0n}}{\dfrac{D}{2} \cdot Q_a} = \dfrac{27924{,}8849}{\dfrac{1.21}{2} \cdot 200000} = 0{,}23$).

Polazeći od simulacionog programa prikazanog na slici 5 i činjenice da je ispravljena struja koja se dovodi na vučne motore određena sledećimizrazom [3,6]:

$$\mathrm{i_a}(\mathrm{t}) = I_{asr}(1 + \lambda \cos 2\omega t) \ldots (17)$$

gde je: I_{asr} - srednja vrednost ispravljene struje vučnog motora;

$\lambda = 0{,}28$ - koeficijent talasnosti ispravljene jednosmerne struje [3,6]

$2\omega = 628\dfrac{rad}{s}$ - kružna učestanost naizmenične komponete ispravljene talasaste struje [2,3,6];

dobijena je zavisnost torzionog momenata na dužem odnosno kraćem delu pogonske osovine prikazana je na slikama 6 i 7.

Starting from the simulation program shown in Figure 5 and the fact that the rectified current supplied to the traction motors is determined by the following expression [3,6]:

$$i_a(t) = I_{asr}(1 + \lambda \cos 2\omega t) \ldots (17)$$

where: I_{asr} - the mean value of the rectified current of the electric motor;

$\lambda = 0{,}28$ - ripple coefficient of rectified direct current,

$2\omega = 628\dfrac{rad}{s}$ - circular frequency of the alternating component of the rectified wave current

the dependence of the torsion moment on the longer and shorter part of the drive shaft is shown in Figures 6 and 7.

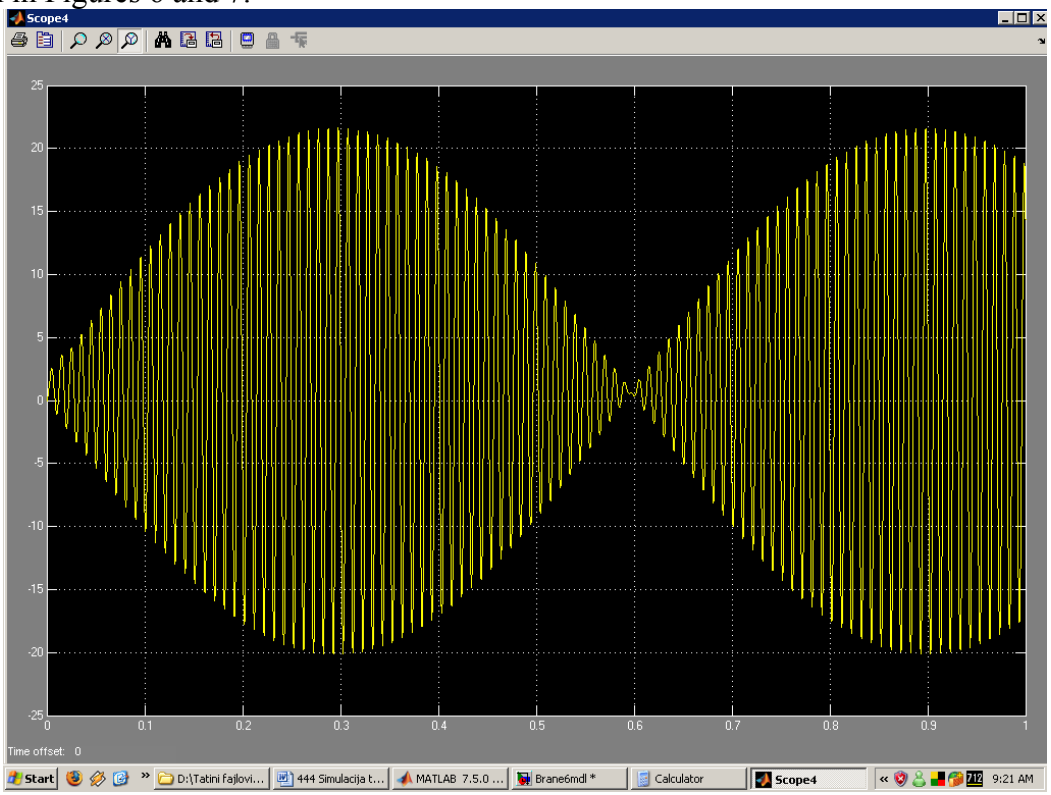

Fig. 6: Dependence $\dfrac{M_{t1}}{M_{0n}} = f(t)$ when slipping on the part of the drive shaft between the large gear and the further monobloc wheel

On the basis of Figure 6 and 7, it can be concluded that when the axle assembly of diode locomotives slips, the torsional moment on the part of the drive shaft between the large gear and the further or closer monoblock wheel increases very quickly. In a short time interval ($t \le 0{,}3s$), this moment reaches the value: $\dfrac{M_{t1}}{M_{0n}} = \dfrac{M_{t2}}{M_{0n}} = 23$ ($M_{t1} = M_{t2} = 6{,}42MNm$) and can lead to permanent damage to these parts of the shaft.

Given that the longer part of the shaft is designed for lower, and the shorter part of the shaft for higher permissible torques, it is obvious that already in the time interval $t \le 0{,}3s$ there is an exceptional risk of breaking only the longer drive shaft. It is clear that in the case of slower anti-skid protection and a longer duration of axle assembly slippage, the risk of breakage and a shorter part of the drive shaft becomes more and more certain [5].

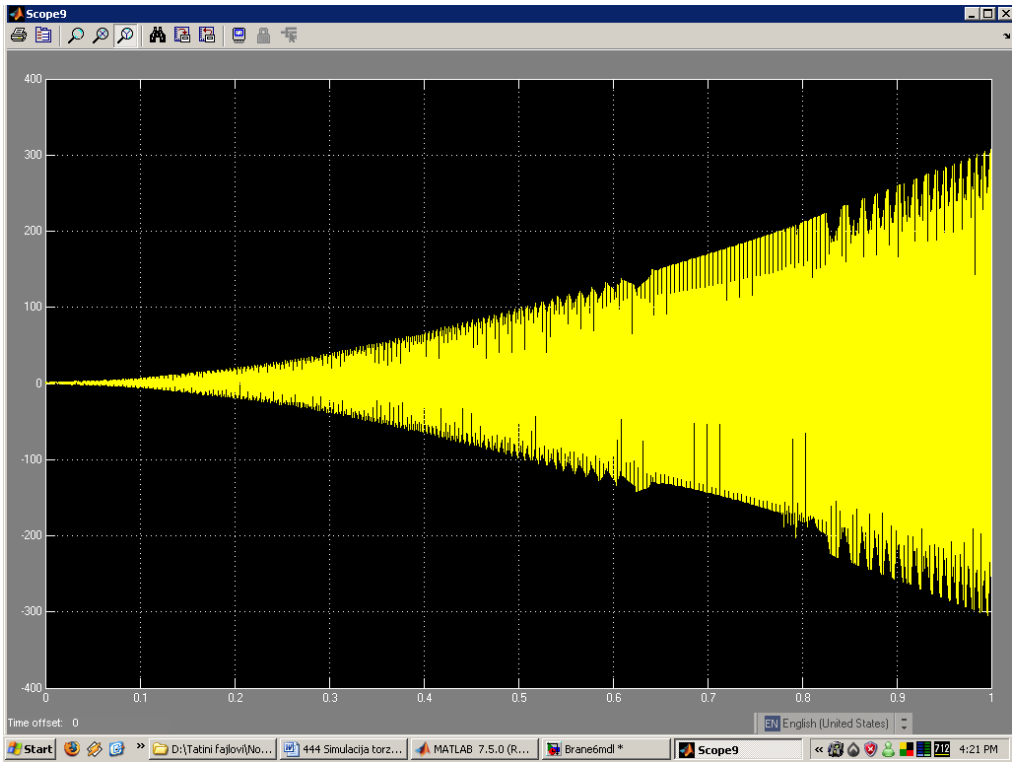

Fig. 7: Dependence $\frac{M_{t2}}{M_{0n}} = f(t)$ when slippig on the part of the drive shaft between the large gear and the closer monobloc wheel

The existing anti-slip protections in diode electric locomotives of "Serbian Railways", such as locomotives of the ŽS 441 series, despite a number of modifications, are quite inert and ineffective. This is because all modifications (even those on ŽS 444 series locomotives) are based on different principles of skid detection and on protective measures which were reduced to reducing the traction force and increasing the friction between the wheel and the rail. Despite all the modifications on the locomotives of the ŽS 444 series, the effective response of these protections remained debatable due to their response time, which is longer than $0{,}3s$.

In order to achieve effective anti-slip protection, research shows that if, in addition to all the above-mentioned protection measures, the degree of current ripple is reduced by using thyristor rectifiers, chokes and permanent shunts of traction motors to the extent that the amplitude factor of the torque harmonics of the circular frequency $2\omega = 628\frac{rad}{s}$ becomes $\lambda = 0{,}1$ dependent $\frac{M_{t1}}{M_{0n}} = f(t)$ it would be like in Figure 8.

On the basis of Figure 8, it is concluded that with a smaller wave of DC rectified current than the existing one, i.e. by reducing $\lambda = 0{,}28$ at $\lambda = 0{,}1$ by using tyristor rectifier or by increasing the inductance of the main locomotive choke, the increase in torsional moment M_{t1} during slippage would decrease almost 5 times compared to the torsional moment in existing locomotives.

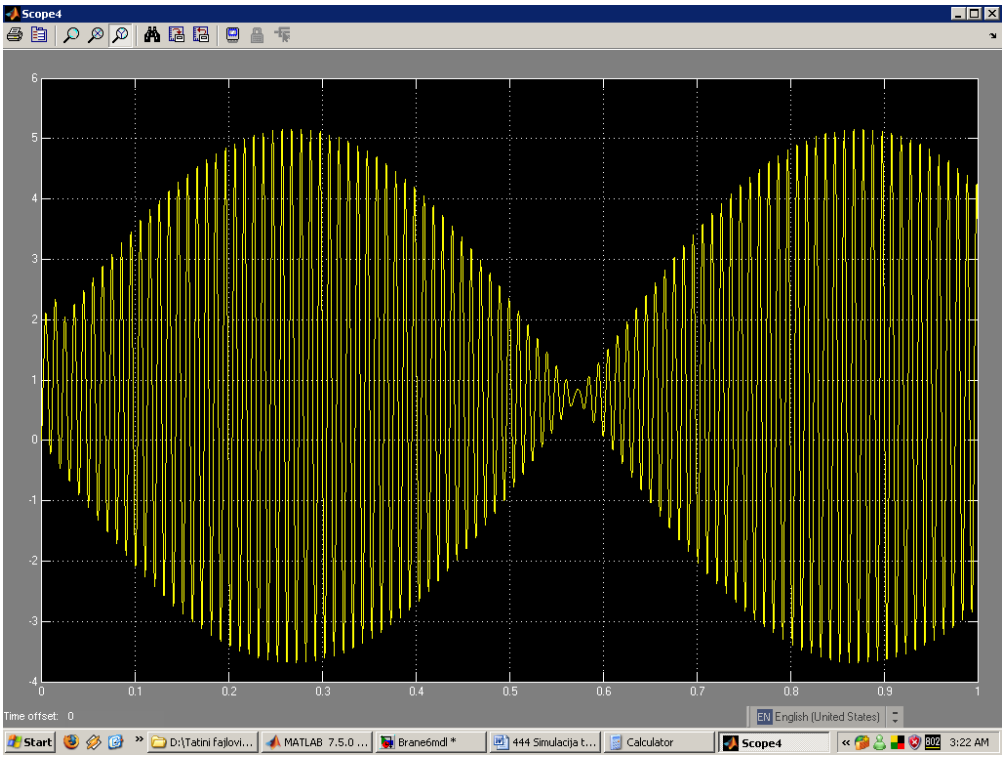

Fig. 8: Dependence $\frac{M_{t1}}{M_{0n}} = f(t)$ when slipping on the part of the drive shaft between the large gear and the further monobloc wheel if $\lambda = 0{,}1$

With the proposed reduction in the degree of ripple of the rectified current, due to the high stiffness of the shorter part of the drive shaft, the dependency $\frac{M_{t2}}{M_{0n}} = f(t)$ during slippage would remain almost unchanged.

In the end, it should be pointed out that until now the influence of the degree of ripple of the DC rectified current of traction electric motors on the effective operation of anti-slip protection of locomotives with DC traction drive has not been analyzed. Therefore, it can be said that the results of these studies show that with the same anti-skid protection, but with the achievement of a lower degree of ripple of the direct current of the traction motors, significantly lower values of torsional oscillations can be achieved when the locomotive shaft slips, and thus a more effective effect of the existing anti-skid protection. This also means that in addition to the problem of timely detection of slippage of locomotive axles with the rail, reduction of the voltage of the traction motors and thus traction forces, as well as appropriate sandblasting between the wheel and the rail, care must also be taken to ensure that the degree of ripple of the direct current of the traction motors is as low as possible. For this reason, electric locomotives that use fully controllable thyristor rectifier bridges, but also an increase in the inductance of the main locomotive choke, are proposed. The use of modern controllable thyristor circuits instead of diode ones can be fully justified if it is known that with the use of thyristor circuits, recuperative braking of the locomotive can also be achieved, i.e. recuperation and return of electrical energy to the contact network.

CONCLUSION

Anti-skid protection of electric locomotives with DC traction motors for wave current, such as locomotives of the ŽS 444 series, is in principle slightly different from this protection in other locomotives. This protection is mainly based on the timely detection of slippage by means of appropriate sensors, the automatic weakening of the traction forces of the drive axles and the increase of adhesion conditions by sandblasting between the wheel and the rail. However, despite the series of locomotive shaft breaks, previous research has not given a precise answer as to how effective anti-slip protection is and for what period of time it must react. The simulation model of the axle assembly of the ŽS 444 series electric locomotive shows that with this locomotive, when the wheel and rail slip, torques 23 times higher than their nominal value can appear in just 0.3 seconds. Values this large can, and in practice this has already been confirmed due to the sluggishness of the anti-skid protection, lead to the breakage of a longer part of the locomotive shaft from the large gear to the monobloc wheel of the locomotive

Reducing the degree of ripple of the rectified direct current of the traction motors significantly improves the operating conditions of the locomotive. Therefore, it is suggested that locomotives using DC wave current electric motors use symmetrical thyristor converters instead of diode rectifiers. This is all the more so since with this change not only less torsional oscillations of locomotive shafts are achieved, i.e. more effective existing anti-slip protection, but also the possibility of choosing locomotive transformers without slow and inefficient step switches, as well as the possibility of installing a more economical recuperative electric brake instead of the existing resistive electric brake.

LITERATURE:

[1] B. Vabić, I Grašković, Tečaj za servisno osoblje lokomotiva serije JŽ 444 i JŽ 461-200, Končar-električne lokomotive dd., broj dokumenta GO5926, lokacija u arhivi 211-0103., Zagreb, 2005.

[2] Dragan B. Rajković: „Prilog analizi loma osovina na lokomotivama serije 441, 461 i 444, Zbornik radova XIV ŽELKON ’10 Niš,strane 193-196, 07-08.oktobar 2010.

[3] R. Jovanović: *«Naponsko stanje lokomotivskih vratila u eksploatacionim uslovima»,* Doktorska disertacija, Mašinski fakultet, Beograd, 1978.

[4] R. Jovanović: «Uzroci, pojave i mogućnosti otklanjanja naprslina i lomova pogonskih osovina (vratila) šinskih vozila», Istraživački projekat RO MIN, Institut „Edvard Kardelj“, Niš, 1987.

[5] Simo Janjanin: „Utvrđivanje uzroka torzionih oscilacija pogonskog sistema lokomotiva 441 simuliranjem sistema na analognom računarskom stroju“, Zajednica Jugoslovenskih Željeznica, Studija, Zagreb, 1974.

[6] Gavrilovic S. Branislav: ”Rotating momentum of the traction electromotor of the thyristoring locomotives series JŽ 444” , 5th International Scientific Conference on Production Engineering, Scientific Book pp. 553-558, ISBN 99589262-0-2, Bihac, BIH, 14-17 Septembar, 2005.

[7] Gavrilovic Branislav: „Research and Analysis in the Electric Traction System of the Serbian Railways“, Eliva Press, SRL, Bd. Moscova 21, Chisinau 2068, Republic of Moldova, Europe,ISBN 9789994986194, 2023.

[8] Ion Boldea, Syed A. Nasar: Electric Drives, 3rd Edition, CRC Press, ISBN 9781032339955, 2017

[9] Nondahl, Thomas A.: „Microprocessor Control of Motor Drives and Power Converters, tutorial course“, IEEE Industry Application Society, pp. 7.1-7.26. October 1993,

[10] Bolton, W. Mechatronics: „Electronic Control Systems in Mechanical and Electrical Engineering“, 3rd edition Pearson Education, 2004.
[11] Harpreet Kaur : „Electric drives and their controlling techniques“, Scholar's press London , Edition: 1, ISBN: 978-613-8-83238-6, London, 2019
[12] Ned Mohan, Siddharth Raju: „Analysis and Control of Electric Drives: Simulations and Laboratory Implementation“ Book, Print ISBN: 9781119584537, Online ISBN: 9781119584575, DOI:10.1002/978111958457, © 2021 John Wiley & Sons, Inc.
[13] Adel Merabet: „Advanced Control Systems for Electric Drives“Published: ISBN 978-3-03943-699-6 (hardback); ISBN 978-3-03943-700-9 (PDF), December 2020, © 2020 by the authors; CC BY-NC-ND licence, https://doi.org/10.3390/books978-3-03943-700-9
[14] Cheku Dorji: „Review Of Electric Motor Drives, Machine Drives and control“, November 2012, DOI: 10.13140/RG.2.1.1198.6408. 2012
[15] Golnaraghi F., Kuo B.C.: „Automatic Control Systems“, 9th ed., 930 pp., John Wiley and Sons Inc., Hoboken, N.J., USA, 2010
[16] .O.V. Kryukov, D.A. Blagodarov, N.N. Dulnev, A.A. Kostin, „Intelligent Control of Electric Machine Drive Systems“, X International Conference on Electrical Power Drive Systems (ICEPDS), 978-1-5386-4713-4/18/$31.00 ©2018 IEEE, 2018
[14] Hughes A.: „Electric Motors and Drives – Fundamentals“, Types and Applications, 3rd ed., 430 pp., Elsevier, Oxford, UK, 2006
[15] Schröder D.: „Elektrische Antriebe – Grundlagen“, 3rd ed., 750 pp., Springer-Verlag, Berlin, Germany, 2007
[16] Christian Jauch , Santhosh Tamilarasan, Katherine Bovee , Levent Güvenc, Giorgio Rizzoni: „Modeling for drivability and drivability improving control of HEV“, Control Engineering Practice 70, 2018,
[17] N. Ramachandran, R. Sivasubramanian, R. Palanivel, P. Nishanth Kalathil, B. Nirmal, "Design and Fabrication of Hybrid Mobility Scooter", *Advances in Materials Research*, vol.5, pp.645, 2021.
[18] Abdul Malek Saidina Omar, Ahmad Asri Abd Samat, Siti Sarah Mat Isa, Sarah Addyani Shamsuddin, Nur Fadhilah Jamaludin, Muhammad Farris Khyasudeen, "New model of inverting substation for DC traction with regenerative braking system", vol.1875, pp.030016, 2017.
[19] Grażyna Barna: „Simulation model of a series DC motor for traction rail vehicles“, Processing of 21st International Conference on Methods and Models in Automation and Robotics (MMAR), Poznan, Poland, 2016, DOI: **10.1109/MMAR.2016.7575192**
[20] Litovchenko, V.V., Nazarov, D.V. & Sharov, V.A. Simulation Model of a Direct-Current Electric Locomotive with Commutator Traction Motors. *Russ. Electr. Engin.* **91**, 69–76 (2020). https://doi.org/10.3103/S1068371220010071
[21] Wang, X., Peng, T., Wu, P., Cui, L. „Influence of electrical part of traction transmission on dynamic characteristics of railway vehicles based on electromechanical coupling model, Scientific Reports, vol., 11, no 1, pp. 1-22, 2021.
[22] Goolak, S., Tkachenko, V., Bureika, G., Vaičiūnas, G.: „Method of spectral analysis of traction current of AC electric locomotives, Transport, vol. 35, no 6, pp. 658-668, 2020.
[23] Litovchenko, V.V., Nazarov, D.V. Sharov, V.A.: „Simulation Model of a Direct-Current Electric Locomotive with Commutator Traction Motors, Russ. Electr. Engin, vol. 91, pp. 69–76, 2020.
[24] Goolak, S., Sapronova, S., Tkachenko, V., Riabov, I., Batrak ,Y.: „Improvement of the model of power losses in the pulsed current traction motor in an electric locomotive, Eastern-European Journal of Enterprise Technologies, vol. 6, no 5(108), pp. 36-46, 2020.

[25] Chiriac, G., Nituca, C., Sticea, D.: „Electric Locomotive Laboratory Test Bench for Research and Educational Purposes, In 2019 8th International Conference on Modern Power Systems (MPS, pp. 1-4. IEEE), 2019.
[26] Goolak, S., Yermolenko, E., Tkachenko, V., Sapronova, S., Yurchenko, V.: „Determination of Voltage at the Rectifier Installation of the Electric Locomotive Vl-80K for Each Position of the Controller Driver's", Technology Audit and Production Reserves, vol. 1, no 1(63), pp 23-29, 2022.
[27] Goolak S., Riabov I., Tkachenko V, Yeritsyan B.: „Simulation model of traction electric drive of AC electric locomotive equipped with collector electric motors, PRZEGLĄD ELEKTROTECHNICZNY, pp. 118-127. ISSN 0033-2097, R. 99 NR 4/2023, doi:10.15199/48.2023.04.21